Food & Function

Accepted Manuscript

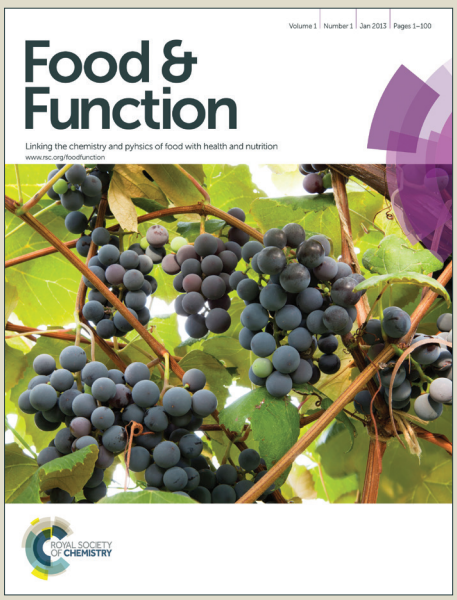

This is an *Accepted Manuscript*, which has been through the Royal Society of Chemistry peer review process and has been accepted for publication.

Accepted Manuscripts are published online shortly after acceptance, before technical editing, formatting and proof reading. Using this free service, authors can make their results available to the community, in citable form, before we publish the edited article. We will replace this *Accepted Manuscript* with the edited and formatted *Advance Article* as soon as it is available.

You can find more information about *Accepted Manuscripts* in the Information for Authors.

Please note that technical editing may introduce minor changes to the text and/or graphics, which may alter content. The journal's standard Terms & Conditions and the Ethical guidelines still apply. In no event shall the Royal Society of Chemistry be held responsible for any errors or omissions in this *Accepted Manuscript* or any consequences arising from the use of any information it contains.

ROYAL SOCIETY OF CHEMISTRY

www.rsc.org/foodfunction

Table of Contents

TOC Graphic

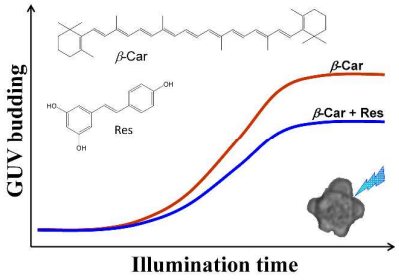

TOC Text

β-Carotene and *trans*-resveratrol protect biomembrane from oxidative stress synergistically, where *β*-carotene induces lag phase and *trans*-resveratrol reduces liposomal budding rate.

Nutritional aspects of *β*-carotene and resveratrol antioxidant synergism in giant unilamellar vesicles

Revision: MS ID FO-ART-03-2014-000225

Hui-Jing Wang,[†] Ran Liang,[*,†] Li-Min Fu,[†] Rui-Min Han,[†] Jian-Ping Zhang,[*,†] Leif H. Skibsted[‡]

[†]*Department of Chemistry, Renmin University of China, Beijing 100872, China*

[‡]*Food Chemistry, Department of Food Science, University of Copenhagen, Rolighedsvej 30, DK-1958 Frederiksberg C, Denmark*

*Authors to whom correspondence should be addressed.

Dr. Ran Liang

E-mail: rliang06@ruc.edu.cn; Tel: +86-10-62516604; Fax: +86-62516444

Prof. Jian-Ping Zhang

E-mail: jpzhang@chem.ruc.edu.cn; Tel: +86-10-62516604; Fax: +86-10-62516444.

Abstract

Giant unilamellar vesicles of soy phosphatidylcholine are found to undergo budding when sensitized with chlorophyll *a* ([phosphatidylcholine]:[chlorophyll *a*]=1500:1) under light irradiation (400−440 nm, 16 mW/mm^2). 'Entropy' as a dimensionless image heterogeneity measurement is found to increase linearly with time during an initial budding process. For *β*-carotene addition ([phosphatidylcholine]:[*β*-carotene]=500:1), a lag phase of 23 s is observed, followed by a budding process at an initial rate lowered by a factor of 3.8, whereas resveratrol ([phosphatidylcholine]:[resveratrol]=500:1) has little if any protective effect against budding. However, resveratrol, when combined with *β*-carotene, is found to further reduce the initial budding rate by a total factor of 4.7 exhibiting synergistic antioxidation effects. It is also interesting that *β*-carotene alone determines the lag phase for initiation of budding while resveratrol supports *β*-carotene in reducing the rate of budding process following the lag phase but it alone has no observable effect on the lag phase. Resveratrol is suggested to regenerate *β*-carotene following its sacrificial protection of unsaturated lipids from oxidative stress, modeling synergistic effects in cell membranes by combinations of dietary antioxidants.

Keywords: antioxidant synergism, *β*-carotene, giant liposome budding, *trans*-resveratrol, membrane integrity

Abbreviations Used

AUC, area under curve; *β*-Car, all-*trans*-*β*-carotene; Chl*a*, chlorophyll *a*; *E*, image entropy; GUV, giant unilamellar vesicle; LP, lag phase; PBS, phosphate buffer solution; PC,

42 L-α-phosphatidylcholine; ROI, region of interest; Res, *trans*-resveratrol; $^1O_2$, singlet oxygen

43

44

Introduction

Oxidative stress is recognized as a threat to human health in relation to exposure to environmental pollution and consumption of processed foods [1,2]. Membranes are organizing biological systems but are sensitive to oxidative damage, which is further detrimental to cellular integrity and function unless repaired [3]. Dietary supplementation with single exogenous antioxidant such as β-carotene (β-Car) in high dosage was, however, found to exhibit adverse effect on human health [4], suggesting that antioxidant interaction is important for optimal protection of membranal integrity and function. A balance between individual antioxidants, as found in many foods of vegetarian origin, therefore seems essential in order to maximize the protective effect [5–7].

Carotenoids are efficient singlet oxygen ($^1O_2$) quenchers protecting against light-induced oxidative damage as in the skin and eye tissues and they are also good radical scavengers [8]. Moreover, there is increasing experimental evidence for synergistic antioxidant interaction between carotenoids and electron-donating antioxidants such as plant polyphenol anions [9–11]. Such antioxidant synergism is often the results of regeneration of a chain-breaking antioxidant by other antioxidants that are less efficient under the actual conditions [12]. For such synergistic antioxidant regeneration in heterogeneous systems, the regenerating antioxidant needs to be more reducing than the regenerated one serving as the primary active antioxidant in the lipid phase. Notably, lipid-water partitioning properties of the interacting antioxidants are also important for efficient regeneration [11].

Liposomes are vesicles composed of lipid bilayers made from phospholipids or other amphiphiles. In recent studies, liposomes are widely used as vehicle for drug delivery [13] and for simulation of

cellular membrane structure and tissue function [14–16]. Giant unilamellar vesicles (GUVs), with typically 5−200 μm diameters, are composed of single lipid bilayer and are found to undergo a variety of 'cytomimetic' morphological transformations such as fusion, fission and budding [17–19]. Such transformations can be directly monitored using optical microscopy, as GUVs equal or exceed cellular dimensions [20–22].

Fluorescence microscopy combined with digital image processing techniques has enabled direct visualization of morphological changes of GUVs [23,24]. For GUVs composed of naturally occurring phospholipids, photo-induced chemical reactions of unsaturated fatty acids such as polymerization and (per)oxidation are suggested to cause morphological changes such as budding [25–28]. Formation of hydroperoxides [29] as the primary oxidation products of unsaturated fatty acids is thus proposed to initiate changes in molecular polarity, leading to surface tension and curvature change and eventually to phase separation and budding [30]. Taking advantage of digital image processing techniques, such microscopic observation at the single liposome level facilitates analysis of heterogeneities in the shape and the size of individual GUVs.

The present study was designed to investigate the antilipoxidation activities of *β*-Car as a carotenoid and *trans*-resveratrol (Res) as an important non-flavonoid plant polyphenol, as well as their possible antioxidant interaction, at the level of single GUV. It is also of relevance to the fields of skin protection from sunlight, since supplementation of both *β*-Car and Res in the skin was found to increase dermal defense against ultraviolet irradiation [31,32], and there are also studies carried out to optimize the bioavailability of the two antioxidant nutrients [33,34]. *β*-Car is readily absorbed

especially from lipid-rich, processed food, and is important both as a pro-vitamin A and as an antioxidant [7,33]. Res has a high bioavailability following oral absorption resulting in blood levels of up to several μmol/L when in a soluble form in food and beverages [34]. Still, their interaction as antioxidants in membranes affecting human health is largely unexplored. The results of present works should also be of relevance as a more generalized data analysis method for other microscopy-related imaging techniques. The present study is based on a novel strategy to investigate interaction of different dietary antioxidants, allowing direct quantification of antioxidant synergism in membranal structures under oxidative stress.

Experimental

Chemicals and Liposome Preparation. Soybean L-*α*-phosphatidylcholine (PC, 23%) and all-*trans*-*β*-carotene (*β*-Car, >95%) were purchased from Sigma Aldrich (St. Louis, MO, USA). *trans*-Resveratrol (Res, >98%) was purchased from Shaanxi Huike Botanical Development Co. Ltd. (Xi'an, China). Chlorophyll *a* (Chl*a*, >95%) was extracted from fresh spinach leaves (see **Figure S1** for details, Supporting Information). Any AR grade organic solvents and inorganic reagents used were purchased from Beijing Chemical Works (Beijing, China), among which chloroform was passed through an Al_2O_3 column and redistilled before use. Methanol (HPLC grade) was purchased from J&K Scientific Ltd. (Beijing, China). Ion-exchanged water was prepared using a Milli-Q Academic Water Purification System (Millipore Corp., Billerica, MA, USA).

Giant unilamellar vesicles (GUVs) were prepared using reverse phase evaporation method originally based on ref (35) with certain modifications as described elsewhere [36]. Briefly, *β*-Car

predissolved in chloroform and Res predissolved in methanol (both 10^{-4} M) were optionally added to methanol/chloroform binary solutions (1:6.7 v/v) of PC (2 mM). Chl*a* predissolved in methanol (10^{-5} M) was added as photosensitizer when needed. The final molar ratio of PC and Chl*a* was 1500:1, and that of PC and antioxidants (β-Car and/or Res) was 500:1. Phosphate buffer solution (PBS, 30 mL, pH 7.4) was slowly added along the flask wall. Organic solvents were then removed by gentle rotary evaporation, yielding an opalescent suspension of GUVs with a volume of approximately 34 mL.

Fluorescence Microscopy and Digital Image Processing. The fluorescence microscopy experiment setup using Eclipse TE-2000U inverted microscope (Nikon Corporation, Tokyo, Japan) and 40× magnifying objective lens (numerical aperture 0.6, CFI Plan Fluor. ELWD, Nikon) is described elsewhere [36]. Briefly, 400−440 nm radiation from an ultra-high pressure mercury lamp with a power density of 16 mW/mm^2 was used for excitation (**Figure S2**, Supporting Information). The GUV images were detected by a Cascade II 512 CCD (Photometrics Inc., Tucson, AZ) and collected by MetaMorph program package (Molecular Devices, Inc., Sunnyvale, CA, USA). 200 μL of liposome suspension was added to a Costar 24-well cell culturing cluster (Corning Incorporated, Corning, NY, USA) placed on the translational stage. Each preparation was measured independently at least 60 times.

The methodology for digital image processing originally developed by Gonzalez and coworkers [37] is described elsewhere [36]. Programs for digital image heterogeneity analysis were manually coded with MATLAB 7.0 (Math works, Inc., Natick, MA, USA). For each digital image an area of 110 ×

110 pixels centered on the target GUV was selected as the region of interest (ROI). The entropy (*E*) was employed as a statistical scalar measurement of image heterogeneity as described in our previous studies [36].

Results

The soy PC GUVs prepared by reverse phase evaporation had spherical shape when observed using an optical microscope, and those with diameters of 20−25 μm were sampled. The blank, unlabeled samples were stable under blue light irradiation (400−440 nm, 16 mW/mm^2) for up to 60 min and underwent no observable morphological change (**Figure S3**, Supporting Information), as also demonstrated in our previous studies [36]. By contrast, GUVs fluorescently labeled with Chl*a* were found to be sensitive to light irradiation, as morphological changes were clearly observed after 5 s and became more distinct upon increasing irradiation time (**Figure 1**). To establish numerical stability and reliability, statistics over 15 independent experiments was performed for each preparation, as seen in **Figure 2** and **Figure S4**. For each GUV image, the entropy (*E*) of the ROI was taken as a dimensionless, scalar measurement of image heterogeneity. The changes in entropy (ΔE) versus illumination time (*t*) were plotted as seen in **Figure 3** for up to 75 s, combining the experimental results represented individually in **Figure S4**. ΔE was found to increase linearly during an initial budding process and then level off at different entropy levels.

The ΔE-*t* curves were analyzed on the basis of different criteria (cf **Figure 2**): (1) The lag phase (LP), determined as the duration between the initiation of reaction (*t*=0) and the intersection of the tangent of the initial linear budding phase on the ΔE-*t* curves and the time axis; (2) The initial rate

of entropy change, defined as the slope of the Δ*E*-*t* curves during the linear budding phase; (3) The integral area under curves (AUC). For GUVs with Res added, as seen from **Figure 3**, Res by itself had negligible effect on inhibition of photo-induced budding (**Figure 1**), which was also evident from the initial rate, the LP and the AUC parameters listed in **Table 1**. By contrast, the addition of *β*-Car to GUVs resulted in slower photo-induced morphological deformation, and the propagation phase on the Δ*E*-*t* curve was retarded for about 20 s (**Figure 3**). For *β*-Car addition, the initial rate and AUC parameters were found to be reduced by factors of 3.8 and 1.8, respectively. When two antioxidants were added together, each at the same concentration level as when added separately, further reduction in the initial rate and the AUC parameters were observed, although the lag phase was comparable to GUV preparations with *β*-Car added alone as antioxidant, as seen in **Figure 3**. The initial rates of budding and the AUC parameters were reduced by total factors of 4.7 and 3.3 with reference to the Chl*a*-labeled control preparations in absence of any antioxidants.

Discussion

A series of morphological transformations of liposomes such as fusion, fission and budding are related to the growth of domains depending on phase separation in vesicles like GUVs [38,39]. Phase separation, either lateral (within a layer) or vertical (between the bilayer), may occur spontaneously or as results of external stimuli from the physico-chemical environments or of chemical reactions [40]. In principle, two types of intramolecular interactions can be involved separately or simultaneously: changes in interactive forces between the polar/ionic head groups and/or among the nonpolar fatty acid moieties [40]. In our experiments, the pH of the aqueous phase was controlled by the use of PBS with a constant ionic strength, and therefore the changes in interactive forces among head groups

were minimized.

For dilinoleoyl PC as the predominant species in the soy lecithin reagent used in the present study, formation of hydroperoxides as the primary products of photo-induced oxidative stress [29] is suggested to initiate the changes in polarity and steric orientation of unsaturated fatty acid moieties. As shown in our previous studies [36], the optimized geometries of linoleic acid hydroperoxides showed significant increases in dipole moments and accordingly structural distortion of unsaturated fatty acid chain occurred to linoleic acid moieties during oxidation. Changes in polarity and distribution and partitioning properties of lipid molecules upon oxidation are suggested to result in the changes in the interactive forces within the hydrophobic interior of the lipid bilayer, which further lead to phase separation, to the subsequent formation of domains and rafts, and eventually to the initiation of GUV budding [30,40].

The molecular mechanism behind the photo-induced GUV budding of Chl*a*-labeled GUVs may accordingly be described as following, serving as a model for oxidative stress in tissues exposed to light like skin and eye. Chl*a* absorbs light and forms the triplet state through intersystem crossing from the primarily populated singlet excited state. Subsequently, $^1O_2$ is generated from the ground state oxygen ($^3O_2$) by energy transfer from the triplet state Chl*a* [41]. The reactive and diffusive $^1O_2$ may directly attack the C=C bonds of unsaturated fatty acid chains through ene reactions to yield hydroperoxides [29]. Such $^1O_2$-initiated lipoxidation reactions are commonly found in edible oils containing trace chlorophylls during storage under light [42].

199 *β*-Car is a lipophilic antioxidant distributing within the interior of the lipid bilayer and it readily
200 reacts with $^1O_2$ with a rate constant reaching the diffusion controlled limit, i.e. 10^{10} $M^{-1}{\cdot}s^{-1}$ [43,44].
201 Therefore, *β*-Car can effectively compete with PC oxidation reactions occurring in the lipid bilayer.
202 In addition, *β*-Car, like most other carotenoids, also hampers the diffusion of lipid radicals in the
203 lipid layers by reducing the fluidity of membrane [45]. Res, as a partially amphiphilic antioxidant,
204 may quench $^1O_2$ directly with a lower rate constant and affect the membrane fluidity to a smaller
205 degree compared to *β*-Car's effects, both of which may explain the less protective effects of Res as
206 compared to *β*-Car's on the morphological deformation of GUVs (**Figure 3**). This is also supported
207 by the substantially different $^1O_2$ quenching rate constants of the two potential antioxidants in
208 deuterated water (pD 7.4), i.e. 1.0×10^{10} $M^{-1}{\cdot}s^{-1}$ and $(3.2\pm0.7)\times10^{8}$ $M^{-1}{\cdot}s^{-1}$ for *β*-Car and Res,
209 respectively [43,46].
210
211 As seen from **Figure 3** for Chl*a*-labeled GUVs with *β*-Car incorporated, a secondary budding
212 propagation phase starts at about 30 s, and the budding rates defined by $\Delta E/\Delta t$ have values of
213 $(8.5\pm0.6)\times10^{-3}$ and $(6.0\pm0.3)\times10^{-3}$ s^{-1} in absence or presence of Res, respectively. Notably, in the
214 presence of *β*-Car, the GUV budding rate in absence of Res is significantly larger than the rate in
215 presence of Res, which may be attributed to the capability for scavenging the potentially
216 prooxidative *β*-Car oxidation products of Res [43]. After the linear increase phases for the ΔE
217 parameter, the ΔE-*t* curves tend to level off at different entropy levels which seem to depend on the
218 nature of antioxidants, either added alone or in combination. This may at least partially be attributed
219 to the oxidative degradation of Chl*a* as the photosensitizer and therefore the cease of $^1O_2$ formation
220 on further increasing of light exposure time. The partially oxidized lipid molecules then tend to

undergo self-organization to restore the original GUV morphologies (data not shown), and the ΔE-t dependency following longer irradiation time may also depend on other factors like inner filter effects and secondary radical processes and is therefore less predictable.

Interestingly, when β-Car and Res are simultaneously introduced to GUVs, a synergistic antioxidant effect was observed as evidenced by further reduction of the initial budding rate and the AUC parameters (**Figure 3**, **Table 1**). This synergism may be attributed to the reactions between β-Car radical species and partially deprotonated Res as secondary radical processes after the initial formation of hydroperoxides. The C=C bonds in unsaturated lipid molecules are directly vulnerable to $^1O_2$ attack with typical second-order rate constants of 10^4–10^5 $M^{-1}{\cdot}s^{-1}$ [47], which are almost independent on the structure of the unsaturated fatty acid or on the temperature as evident by low activation energies [48]. The initially formed hydroperoxides subsequently undergo homolytic cleavage between the O-O bonds because of the relatively lower O-O bond energies compared to the O-H bonds [49], yielding alkoxy radicals which are very reactive secondary oxidation products of unsaturated fatty acids. β-Car, like many other carotenoids, is capable of scavenging alkoxy radicals via electron transfer to yield the radical cations of the carotenoid [43,44]. The antioxidant synergism between β-Car and Res can therefore be attributed to the electron transfer to β-Car radical cations which results in regeneration of β-Car by Res anion, or to radical adduct formation reactions between β-Car radical cations and partially deprotonated Res, as seen for reactions between carotenoids and polyphenols like (iso)flavonoids and green tea catechins [11,50].

Conclusion

From our studies of giant unilamellar vesicle budding using fluorescence microscopy and digital image processing techniques, we may conclude that *β*-carotene yields protection against photosensitized oxidation in cell membranes as evidenced by appearance of a lag phase for budding. Resveratrol shows little such effect but lowers the rate of budding following the lag phase caused by the presence of *β*-carotene through protection of *β*-carotene from oxidative degradation or through scavenging of prooxidative degradation products of *β*-carotene by its phenolate form.

Acknowledgements

Support from the Fundamental Research Funds for the Central Universities of China (10XNI007) and support from the Danish Research Council for Technology and Production as the grant 09-065906/FTP: Redox communication in the digestive tract are acknowledged.

References

(1) B. Halliwell, Oxidative stress and cancer: Have we moved forward?, *Biochem. J.*, 2007, **401**, 1−11.

(2) N. Singh, A. K. Dhalla, C. Seneviratne and P. K. Singal, Oxidative stress and heart failure, *Mol. Cell. Biochem.*, 1995, **147**, 77−81.

(3) J. Amer, H. Ghoti, E. Rachmilewitz, A. Koren, C. Levin and E. Fibach, Red blood cells, platelets, and polymorphonuclear neutrophils of patients with sickle cell disease exhibit oxidative stress that can be ameliorated by antioxidants, *Br. J. Haematol.*, 2006, **132**, 108−113.

(4) G. S. Omenn, G. E. Goodman, M. D. Thornquist, J. Balmes, M. R. Cullen, A. Glass, J. P. Reogh, F. L. Meyskens, B. Valanis, J. H. Williams, S. Barnhart and S. Hammar, Effects of a combination

of beta carotene and vitamin A on lung cancer and cardiovascular disease, *New Engl. J. Med.*, 1996, **334**, 1150–1155.

(5) P. C. H. Hollman and M. B. Katan, Dietary flavonoids: intake, health effects and bioavailability, *Food Chem. Toxicol.*, 1999, **37**, 937–942.

(6) X. Wu, G. R. Beecher, J. M. Holden, D. B. Haytowitz, S. E. Gebhardt and R. L. Prior, Lipophilic and hydrophilic antioxidant capacities of common foods in the United States, *J. Agric. Food Chem.*, 2004, **52**, 4026–4037.

(7) L. H. Skibsted, Vitamin and non-vitamin antioxidants and their interaction in food, *J. Food. Drug Anal.*, 2012, **20**, Suppl 1, 355–358.

(8) A. Galano, Relative antioxidant efficiency of a large series of carotenoids in terms of one electron transfer reactions, *J. Phys. Chem. B*, 2007, **111**, 12898–12908.

(9) R. M. Han, Y. X. Tian, E. M. Becker, M. L. Andersen, J. P. Zhang and L. H. Skibsted, Puerarin and conjugate bases as radical scavengers and antioxidants: molecular mechanism and synergism with *β*-carotene, *J. Agric. Food Chem.*, 2007, **55**, 2384–2391.

(10) R. Liang, R. M. Han, L. M. Fu, X. C. Ai, J. P. Zhang and L. H. Skibsted, Baicalin in radical scavenging and its synergistic effect with *β*-carotene in antilipoxidation, *J. Agric. Food Chem.*, 2009, **57**, 7118–7124.

(11) R. Liang, C. H. Chen, R. M. Han, J. P. Zhang and L. H. Skibsted, Thermodynamic versus kinetic control of antioxidant synergism between *β*-carotene and (iso)flavonoids and their glycosides in liposomes, *J. Agric. Food Chem.*, 2010, **58**, 9221−9227.

(12) R. M. Han, C. H. Chen, Y. X. Tian, J. P. Zhang and L. H. Skibsted, Fast regeneration of carotenoids from radical cations by isoflavonoid dianions: Importance of the carotenoid keto group

for electron transfer, *J. Phys. Chem. A*, 2010, **114**, 126–132.

(13) V. P. Torchilin, Multifunctional nanocarriers, *Adv. Drug Deliv. Rev.*, 2006, **58**, 1532−1555.

(14) D. Dutta, A. Pulsipher, W. Luo, H. Mak and M. N. Yousaf, Engineering cell surfaces via liposome fusion, *Bioconjugate Chem.*, 2011, **22**, 2423−2433.

(15) D. Dutta, A. Pulsipher, W. Luo, and M. N. Yousaf, Synthetic chemoselective rewiring of cell structures: Generation of three-dimensional tissue structures, *J. Am. Chem. Soc.*, 2011, **133**, 8704−8713.

(16) V. A. Hernandez, G. Karlsson and K. Edwards, Intrinsic heterogeneity in liposome suspensions caused by the dynamic spontaneous formation of hydrophobic active site in lipid membranes, *Langmuir*, 2011, **27**, 4873−4883.

(17) F. M. Menger and K. D. Gabrielson, Cytomimetic organic chemistry: Early developments, *Angew. Chem. Int. Ed. Engl.*, 1995, **34**, 2091−2106.

(18) F. M. Menger and J. S. Keiper, Chemistry and physics of giant vesicles as biomembrane models, *Curr. Opin. Chem. Biol.*, 1998, **2**, 726−732.

(19) F. M. Menger and V. A. Azov, Cytomimetic modeling in which one phospholipid liposome chemically attacks another, *J. Am. Chem. Soc.*, 2000, **122**, 6492−6493.

(20) L. A. Bagatolli, To see or not to see: Lateral organization of biological membranes and fluorescence microscopy, *Biochim. Biophys. Acta*, 2006, **1758**, 1541−1556.

(21) B. L. Stottrup, A. H. Nguyen and E. Tüzel, Taking another look with fluorescence microscopy: Image processing techniques in Langmuir monolayers for the twenty-first century, *Biochim. Biophys. Acta*, 2010, **1798**, 1289−1300.

(22) N. F. Morales-Penningston, J. Wu, E. R. Farkas, S. L. Goh, T. M. Konyakhina, J. Y. Zheng, W.

W. Webb and G. W. Feigenson, GUV preparation and imaging: Minimizing artifacts, *Biochim. Biophys. Acta*, 2010, **1798**, 1324−1332.

(23) D. M. Haverstick and M. Glaster, Visualization of Ca^{2+}-induced phospholipid domains, *Proc. Natl. Acad. Sci.USA*, 1987, **84**, 4475−4479.

(24) D. M. Haverstick and M. Glaster, Visualization of domain formation in the inner and outer leaflets of a phospholipid bilayer, *J. Cell Biol.*, 1988, **106**, 1885−1892.

(25) J. Zhao, J. Wu, H. Shao, F. Kong, N. Jain, G. Hunt and G. Feigenson, Phase studies of model biomembranes: Macroscopic coexistence of Lα+Lβ, with light-induced coexistence of Lα+Lo phases, *Biochim. Biophys. Acta*, 2007, **1768**, 2777−2786.

(26) J. Heuvingh and S. Bonneau, Asymmetric oxidation of giant vesicles triggers curvature-associated shape transition and permeabilization, *Biophys. J.*, 2009, **97**, 2904−2912.

(27) A. G. Ayuyan and F. S. Cohen, Lipid peroxides promote large rifts: Effects of excitation of probes in fluorescence microscopy and electrochemical reactions during vesicle formation, *Biophys. J.*, 2006, **91**, 2172−2183.

(28) K. Ishii, T. Hamada, M. Hatakeyama, R. Sugimoto, T. Nagasaki and M. Takagi, Reversible control of *exo*- and *endo*-budding transitions in a photosensitive lipid membrane, *ChemBioChem*, 2009, **10**, 251−256.

(29) E. Choe and D. B. Min, Chemistry and reactions of reactive oxygen species in foods, *Crit. Rev. Food Sci. Nutr.*, 2006, **46**, 1−22.

(30) E. Farge and P. F. Devaux, Shape changes of giant liposomes induced by an asymmetric transmembrane distribution of phospholipids, *Biophys. J.*, 1992, **61**, 347−357.

(31) W. Stahl and H. Sies, *β*-Carotene and other carotenoids in protection from sunlight, *Am. J. Clin.*

Nutr., 2012, **96**, 1179S−1184S.

(32) F. Afaq and H. Mukhtar, Botanical antioxidants in the prevention of photocarcinogenesis and photoaging, *Exp. Dermatol.*, 2006, **15**, 678−684.

(33) N. V. Dimitrov, C. Meyer, D. E. Ullrey, W. Chenoweth, A. Michelakis, W. Malone, C. Boone and G. Fink, Bioavailability of *β*-carotene in humans, *Am. J. Clin. Nutr.*, 1988, **48**, 298−304.

(34) M. J. Amiot, B. Romier, T. M. A. Dao, R. Fanciullino, J. Ciccolini, R. Burcelin, L. Pechere, C. Emond, J. F. Savouret and E. Seree, Optimization of *trans*-resveratrol bioavailability for human therapy, *Biochemie*, 2013, **95**, 1233−1238.

(35) A. Moscho, O. Orwar, D. T. Chiu, B. P. Modi and R. N. Zare, Rapid preparation of giant unilamellar vesicles, *Proc. Natl. Acad. Sci. U.S.A.*, 1996, **93**, 11443−11447.

(36) R. Liang, Y. Liu, L. M. Fu, X. C. Ai, J. P. Zhang and L. H. Skibsted, Antioxidants and physical integrity of lipid bilayers under oxidative stress, *J. Agric. Food Chem.*, 2012, **60**, 10331−10336.

(37) R. C. Gonzalez, R. E. Woods and S. L. Eddins, in *Digital image processing using MATLAB*, Prentice-Hall, Upper Saddle River, NJ, 2nd edn., 2009, ch. 12, pp. 597−673.

(38) R. Lipowsky, Domains and rafts in membranes – hidden dimensions of selforganization, *J. Biol. Phys.*, 2002, **28**, 195−210.

(39) F. Julicher and R. Lipowsky, Domain-induced budding of vesicles, *Phys. Rev. Lett.*, 1993, **70**, 2964−2967.

(40) W. H. Binder, V. Barragan and F. M. Menger, Domains and rafts in lipid membranes, *Angew. Chem. Int. Ed.*, 2003, **42**, 5802−5827.

(41) A. Krieger-Liszkay, Singlet oxygen production in photosynthesis, *J. Exp. Bot.*, 2004, **56**,

353 337−346.

354 (42) D. B. Min and J. M. Boff, Lipid oxidation of edible oil, in *Food Lipids*, ed. C. C. Akoh and D.

355 B. Min, Marcel Dekker Inc., New York, 2002, pp. 335−364.

356 (43) F. Böhm, R. Edge and G. Truscott, Interactions of dietary carotenoids with activated (singlet)

357 oxygen and free radicals: Potential effects for human health, *Mol. Nutr. Food Res.*, 2012, **56**,

358 205−216.

359 (44) A. Cantrell, D. J. McGarvey, T. G. Truscott, F. Rancan and F. Böhm, Singlet oxygen quenching

360 by dietary carotenoids in a model membrane environment, *Archives Biochem. Biophys.*, 2003, **412**,

361 47−54.

362 (45) J. Liang, Y. X. Tian, F. Yang, J. P. Zhang and L. H. Skibsted, Antioxidant synergism between

363 carotenoids in membranes. Astaxanthin as a radical transfer bridge, *Food Chem.*, 2009, **115**,

364 1437−1442.

365 (46) J. A. Celaje, D. Zhang, A. M. Guerrero and M. Selke, Chemistry of *trans*-resveratrol with

366 singlet oxygen: [2+2] addition, [4+2] addition, and formation of the phytoalexin moracin M, *Org.*

367 *Lett.*, 2011, **13**, 4846−4849.

368 (47) C. Vever-Bizet, M. Dellinger, D. Brault, M. Rougee and R. V. Bensasson, Singlet molecular

369 oxygen quenching by saturated and unsaturated fatty-acids and by cholesterol, *Photochem.*

370 *Photobiol.*, 1989, **50**, 321−325.

371 (48) W. T. S. Yang and D. B. Min, Chemistry of singlet oxygen oxidation of foods, in *Lipids in*

372 *Food Flavors*, ed. C. T. Ho and T. G. Hartmand, American Chemistry Society, Washington: DC,

373 1994.

374 (49) R. R. Hiatt, T. Mill and F. R. Mayo, Homolytic decompositions of hydroperoxides. I. Summary

and implications for autoxidation, *J. Org. Chem.*, 1968, **33**, 1416−1420.

(50) L. L. Song, R. Liang, D. D. Li, Y. D. Xing, R. M. Han, J. P. Zhang and L. H. Skibsted, *β*-Carotene radical cation addition to green tea polyphenols. Mechanism of antioxidant antagonism in peroxidizing liposomes, *J. Agric. Food Chem.*, 2011, **59**, 12643−12651.

381 **Table 1.** Lag phase, initial rate and area under curve (AUC in arbitrary units) of Δ*E*-*t* curves of

382 fluorescently labeled GUVs exposed to light (400−440 nm, 16 mW/mm^2) for up to 75 s.

383

Sample	Lag Phase / s	Initial Rate / s^{-1}	AUC / a.u.
Control	0.18	$(6.5\pm0.13)\times10^{-3}$	14
Res	2.4	$(6.2\pm0.42)\times10^{-3}$	13
β-Car	23	$(1.7\pm0.27)\times10^{-3}$	7.8
β-Car + Res	24	$(1.4\pm0.44)\times10^{-3}$	4.2

384

385

386

Figure Captions

Figure 1. Digital images of fluorescently labeled GUVs exposed to light (400−440 nm, 16 mW/mm^2) for up to 75 s. Samples: (a) control; (b) Res only; (c) β-Car only; (d) both antioxidants present.

Figure 2. ΔE-*t* curve for fluorescently labeled GUVs with only β-Car added (**Figure 1**(c)) and schematic presentation of statistics and data analysis criteria: the lag phase, the initial rate and the area under curve (AUC). Irradiation starts at time 0 s.

Figure 3. ΔE as a dimensionless scalar measurement of heterogeneity for unlabeled GUVs (blank); labeled GUVs without antioxidants added (control) and labeled GUVs containing at least one antioxidant for up to 75 s. For clarity, error bars are not shown. Irradiation starts at time 0 s.

399 **Figure 1.**

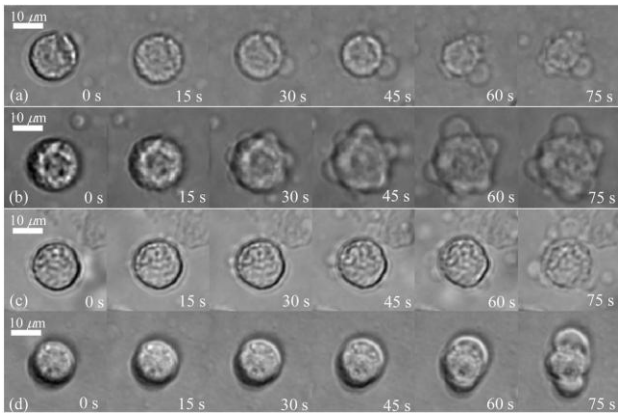

400

401

402

403 **Figure 2.**

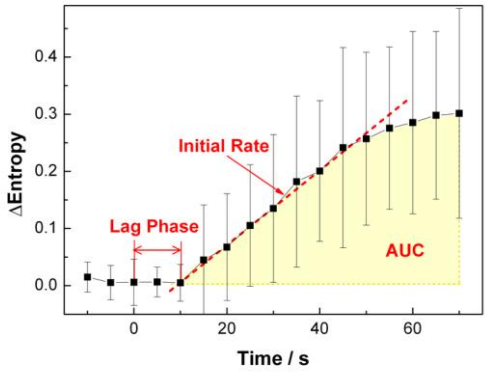

404

405

406

407 **Figure 3.**

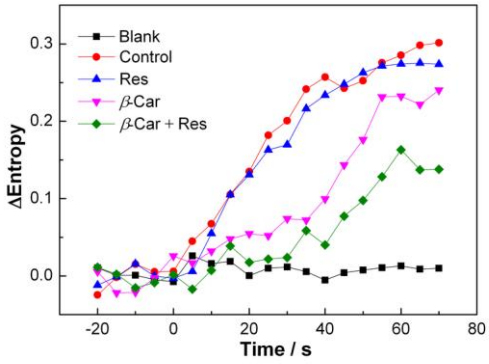

408

409

410

Table of Contents

TOC Graphic

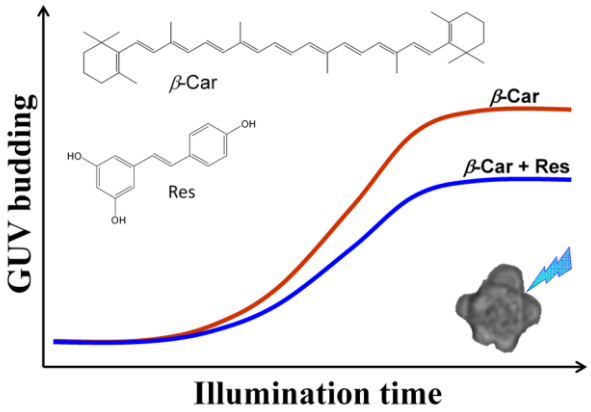

TOC Text

β-Carotene and *trans*-resveratrol protect biomembrane from oxidative stress synergistically, where *β*-carotene induces lag phase and *trans*-resveratrol reduces liposomal budding rate.